The MhLHCB15 gene interacts with interacting proteins to regulate iron deficiency tolerance in Malus halliana

Yongjuan Dong
Gansu Agricultural University
Zhongxing Zhang
Gansu Agricultural University
Jiao Cheng
Gansu Agricultural University
Yanlong Gao
Gansu Agricultural University
Xiaoya Wang
Gansu Agricultural University
Wenbin Zhao
Gansu Agricultural University
Donghai Zhang
Gansu Agricultural University
Yanxiu Wang
wangxy@gsau.edu.cn
Gansu Agricultural University

Research Article

Keywords: functional features, Fe deficiency, MhLHCB15 gene, interacting protein

Posted Date: February 14th, 2024

DOI: https://doi.org/10.21203/rs.3.rs-3951417/v1

Additional Declarations: No competing interests reported.

Abstract

Background

Iron (Fe) plays a crucial role as a micronutrient in facilitating plant growth and development. Alterations in the availability of iron can trigger a response resulting in iron deficiency, ultimately affecting both plant growth and crop yield.

Results

A total of 33 *MhLHC* family members were identified in *Malus halliana* based on the apple genome database under Fe deficiency. The study comprehensively analyzed the physicochemical properties, gene structures, conserved motif compositions, evolutionary relationships, and chromosomal distributions of these family members. Additionally, 15 genes were selected for qRT-PCR to verify whether they responded to abiotic stress. It was demonstrated that *MhLHCB15* significantly responded to Fe deficiency stress. Among them, Further investigation was conducted on the functional properties of *MhLHCB15* in *Arabidopsis* and apple calli. Overexpression of *MhLHCB15* enhanced Fe deficiency tolerance of in both *Arabidopsis* and apple calli, which evoked a variety of biochemical changes: transgenic *Arabidopsis* displayed higher photosynthetic efficiency (Tr, Gs, and Pn) and fluorescence parameters (qP, F0, Fm, and Fv/Fm) and lower Ci compared to the WT. The chlorophyll content, photosynthetic products (SS, St and SP), and enzyme activities (SOD, POD and CAT) of transgenic *A. thaliana* and apple calli were markedly higher compared to the WT, however, the MDA content and ROS accumulation were less than the WT. Moreover, the FCR activity of transgenic *Arabidopsis* and apple calli was stronger in comparison to the WT.

Conclusions

In summary, overexpression of the *MhLHCB15* gene enhanced *Arabidopsis* and apple calli tolerance to Fe deficiency stress. In this study, the interaction proteins *MhSGR1* and *MhTHF1* of *MhLHCB15* were screened, which contributes to further analyze the regulation of *MhLHCB15* on Fe deficiency tolerance of *M. halliana*.

INTRODUCTION

Iron (Fe), a crucial mineral element necessary for the growth and development of plants, is engaged in many important biological processes, including photosynthesis, respiration, redox reactions and nitrogen fixation[1,2]. When there is a deficiency of Fe, it can restrict chlorophyll synthesis, lower the photosynthetic rate, cause leaf chlorosis, and ultimately decrease fruit output and quality[3–5]. While most soils contain sufficient total iron, the availability of iron to plants may be insufficient due to various soil factors. Fe deficiency can occur as a result of high pH and $CaCO_3$ concentration, ionic imbalance,

and inadequate physical qualities such as high or low soil temperature, excessive humidity, poor soil aeration, and compaction, particularly in calcareous soils[6]. And approximately 40% of the world's soils are considered Fe limiting for plant growth[7]. The northwest Loess Plateau region of China is the best ecological zone for apple cultivation[8], the majority of orchards are calcareous soils with serious soil salinization, which have resulted in the lower solubility of iron and nutrient deficiency[9]. Hence, Fe depletion severely constrained apple production in the region. To derive adequate iron for survival, plants have evolved a range of mechanisms to improve their ability to obtain iron from the soil[10,11]. The plants tightly control Fe uptake, translocation and storage to maintain Fe homeostasis at the whole-plant level[1,12].

Photosynthesis serves as the foundation of life on earth, there are many heme- and Fe-S cluster-containing proteins working in photosynthetic electron transport chain so that iron (Fe) deficiency tends to cause severe photodamage[13]. The primary location of this photodamage occurs in photosystem II (PSII)[14], and hence plants modulate their absorption of light energy by altering the size of the PSII-LHCII light-trapping antennae. The LHC family proteins encoded by nuclear genes act as antennae proteins and are crucial in light energy trapping and energy transfer as well as in response to adversity stresses[15,16]. The LHC gene family mainly consists of two main evolutionary taxa, LHCB and LHCA, which are associated with photosystem I (PSI) and PSII in the photosynthetic system, respectively[17]. The capture and transfer of photosynthetic energy in higher plants is primarily accomplished by the light-harvesting chlorophyll a/b-binding protein (LHCI, LHCII)[18,19]. LHCII, the primary antenna protein present in plant PSII, effectively converts the absorbed light energy into usable form, contributing significantly to plant photosynthesis. It facilitates the transfer and conversion of light energy, which also ensures the proper distribution of vesicle accumulation and excitation between the two photosystems, thereby offering photoprotection and aiding in the adaptation to diverse environmental conditions[20]. The most abundant LHCII, also referred to as the major LHCII, consists of LHCB1, LHCB2, and LHCB3 proteins[21]. Additionally, there are three minor LHCII proteins: LHCB4 (CP29), LHCB5 (CP26), and LHCB6 (CP24)[22,23].

LHCB1 and LHCB2 can modulate the energy homeostasis distribution between PSI and PSII[24–26]. Andersson et al.[27] discovered that LHCB1 and LHCB2 proteins affect photosynthesis, which leads to a decline in light uptake by leaves, and a decrease in chlorophyll content in plants lacking the LHCB1 and LHCB2 genes, whereas plants with a light green coloration. Additionally, numerous LHCII genes have been found to regulate responses to abiotic stress[26,28]. Overexpression of *LeLHCB2* in tomato lessens the accumulation of ROS under low-temperature stress and enhances the low-temperature tolerance of transgenic tobacco[29]. The PSII antenna proteins CP29 and CP47 of Salicornia europaea, as well as several LHCII proteins, showed increased abundance in response to salt treatment, which enhanced the excitation energy capture capacity and efficiency of PSII[30]. The expression of LHCB1 gene in *Oenanthe javanica* was up-regulated under cold and drought stresses, which remarkably elevated photosynthesis[28]. LHCII protein of *Arabidopsis thaliana* also interacts with the Thylakoid Formation 1 (THF1) protein, in which silencing the THF1 gene can mitigate the degradation of LHCII protein and delay the yellowing of plant leaves[31]. In previous studies, SGR1 was shown to specifically interact with LHCII

to minimize the risk of photo-dynamism of these light-excitable intermediates by metabolically channel chlorophyll breakdown pigments, thereby preventing accelerated plant death during leaf senescence[32]. Consequently, LHCII proteins perform an extremely important role in plant photosynthesis.

Malus halliana is a genus of apple native to the arid saline habitats of the Hexi Corridor in Gansu Province and has been found to have certain Fe deficiency tolerance in long-term researches[9,33]. The 33 *MhLHC* family members were screened to analyze them bioinformatically. The qRT-PCR assay indicated that *MhLHC15* markedly responded to Fe deficiency stress. In this experiment, the *MhLHCB15* gene was cloned from *M. halliana*, as well as *MhLHCB15* transgenic apple calli and *A. thaliana* were obtained by gene transformation, which were subjected to Fe-deficiency stress test and the physiological parameters were determined. Furthermore, the yeast two-hybrid (Y2H) technology was used to identify the proteins that interact with *MhLHCB15*, which provided a powerful rationale and reference for the analysis of the biological function of *MhLHCB15* under adversity stress and the construction of the regulatory network.

MATERIAL AND METHODS

Plant material and treatment

The *Malus halliana* plants was regularly transferred every 30 days onto a nutrient-rich solid medium called Murashige and Skoog (MS) at a temperature of 25°C. This medium consisted of 0.5 mg L^{-1} of 6-BA and 0.1 mg L^{-1} of NAA. The solid medium, referred to as MS, comprised of 4.43 g L^{-1} of MS powder obtained from Coolaber, Beijing, China. Additionally, it contained 30 g L^{-1} of sucrose and 7 g L^{-1} of agar, with the pH range of 5.8 to 6.0.

For gene expression analysis, seedlings of *M. halliana* were subcultured for about 20 days in rooting culture medium, composed of 0.5 microelements, 0.5 microelements, 0.4 mg l^{-1} NAA and 7 g L^{-1} agar, pH 5.8-6.0. Once seedlings had developed roots, plants were selected and pre-cultured on MS medium for 7 days. After 7 days of culture, *M. halliana* were subjected to different abiotic stress treatments, which were Fe deficiency (0 μM Fe)[34], drought stress (15% PEG 6000), low temperature (4℃), saline-alkali stress (200 mmol/L NaCl + $NaHCO_3$). Three replicates of each treatment were conducted, with five plants per replicate. We carefully gathered leaves at various time intervals: 0, 12, 24, 48, and 72 hours, and placed in liquid nitrogen in a refrigerator at 80°C for later use.

Yeast strain (Y2H Gold) and yeast medium were purchased from Coolaber Bio Inc. The vectors pGBKT7 and pGADT7 were kindly donated by Prof. Wang Xiaofei from Shandong Agricultural University.

Identification of LHC genes in M. halliana

All the LHC family members were screened from the apple genome database. Subsequently, the transcript IDs were converted to corresponding gene IDs and the corresponding genes were found in the

apple genome. After obtaining the candidate genes, LHC members were further screened and validated using Pfam and SMART databases, ultimately 33 LHC members were identified for subsequent analysis.

Phylogenetic analysis and gene sequence analysis

In order to explore the evolutionary relationship between members of apple *MhLHC* proteins, the phylogenetic tree was constructed based on amino acid sequences of the LHC family from both *Arabidopsis* and *M. halliana*. *Arabidopsis* LHC proteins were retrieved from the TAIR database. The MEGAX software was used to systematically analyze the LHC proteins of *Arabidopsis* and *M. halliana*. Neighbor-Joining (NJ) was employed to predict the phylogenetic tree, which was subjected to a Bootstrap method with 1000 replications. In addition, the physical and chemical properties and hydrophobicity predicted proteins were analyzed using ExPASy online tools (https://web.expasy.org/protparam/ *and* https://web.expasy.org/protscale/*).* We utilized the online tool Plant-mPLoc (http://www.csbio.sjtu.edu.cn/bioinf/Cell-PLoc-2/*)* to predict and analyze the subcellular localization. Additionally, we employed the MEME suite online tool to analyze the conserved protein motifs (https://meme-suite.org/tools/meme*).* Cis-acting promoter elements were predicted and analyzed with the PLACE database (https://www.dna.affrc.go.jp/PLACE*).* Finally, in order to determine chromosome distribution of the apple *MhLHC* gene family, annotation information on the apple genome was downloaded from the Phytozome database and gene distribution visualized with TBtools.

Quantitative real-time PCR

An RNA extraction kit (Accurate Biotechnology (Hunan) Co., Ltd) was utilized to extract total RNA from the samples. Reverse transcription was performed using the *Evo M-MLV* RT Mix kit with gDNA Clean for qPCR (Accurate Biotechnology (Hunan) Co., Ltd). About 1 μg total RNA was transcribed into cDNA. Primers were designed by Shanghai Sangon Biological Engineering (China) based on sequences retrieved from the apple genome database. Real-time PCR primer pairs are listed in Table S1. Real-time PCR was performed using cDNA of *M. halliana* as template. The $2^{-\Delta\Delta Ct}$ method was utilized for quantitative analysis of the data, with *MhGAPDH* and *AtActin* serving as the reference genes for quantitative real-time PCR [35]. The reaction system contained: 10 μl 2×SYBR Green Pro Taq HS (10 μmol l^{-1}), 1 μl upstream primers (10 μmol l^{-1}), 1 μl downstream primers, 2 μl cDNA template and 6 μl RNase free water. The experimental setup included the following reaction parameters: pre-denaturation at 95°C for 30 s, denaturation at 95°C for 5 s, annealing at 60°C for 30 s and extension at 37°C for 5 s, repeated for 50 cycles. Three replicates were performed for each sample.

Gene cloning and vector construction

LHC family members induced by Fe deficiency were identified in the apple genome database and compared to sequences at NCBI (https://www.ncbi.nlm.nih.gov/*)* to obtain the apple *MhLHCB15* (103429652). And then were designed using DNAMAN. Forward Primer: ATGGCAGCTTCCATGGCT and Reverse primer: TCACTTTCCGGGAACAAAG. The PCR product was subjected to electrophoresis on 1% agarose gel to separate the fragments. The targeted gene fragment was then recovered from the gel and ligated with the pMD19-T cloned vector for sequencing. This was then transformed in *E. coli* sequenced

and sieved. The correct sequence of the *MhLHCB15* plasmid was extracted, digested with the restriction enzymes *Sma*Ⅰ and *Kpn*Ⅰ, and connected to the pRI101 expression vector. Next, *E. coli* underwent transformation, and a positive colony was identified, which was further transformed into *Agrobacterium GV3101* using freeze-thaw method for genetic transformation.

The specific primers *MhSGR1* and *MhTHF1* (Table S1) were designed, according to the sequence (103444765, 103411255) retrieved in NCBI database. The cDNA of *M. halliana* was utilized as the template for RT-PCR amplification, and the amplified product was purified and sequenced. The pGADT7 vector was double digested with *EcoR*Ⅰ and *BamH*Ⅰ, and the correctly sequenced PCR purified and recovered products were ligated with the digested products and transformed into *E.coli*, and a single clone was picked for colony PCR detection, and the positive clones were sequenced, and the pGADT7-*MhSGR1* and pGADT7-*MhTHF1* recombinant plasmid was extracted after the correct sequencing.

Agrobacterium-mediated transformation of Arabidopsis thaliana and apple calli

A. thaliana seeds were obtained through genetic transformation following the method described by Hu et al.[36]. The seeds were treated with 75% ethanol for 5 min, followed by a 10 min treatment with 26% sodium hypochlorite. Subsequently, the seeds were rinsed with deionized water three to five times. The resistant plants were screened on MS medium containing 30 mg L^{-1} kanamycin, and heterozygous transgenic plants were obtained. After three successive generations of screening, the homozygous transgenic plants of the T3 generation were obtained.

Infection of apple calli was based on the method of Hu et al.[36]. After 15 days, calli of the same culture state were immersed in infection solution with an OD value of 0.4 to 0.6 cultured in the dark (220 r min^{-1}) for 15–20 min, then filtered. The calli were placed on solid MS medium for 2 days and spread evenly on 250 mg L^{-1} cephalosporin and 30 mg L^{-1} kanamycin resistance medium. They were screened for about 30 days on the plate until the transgenic calli was obtained. Then they were evenly distributed on 250 mg/L cephalosporin and 30 mg/L kanamycin resistant medium for 3–5 times to obtain stable growth resistant calli. DNA was extracted and used for PCR identification.

Treatment with Fe deficiency in A. thaliana and apple calli and physiological index measurement

The seeds of the wild-type (WT) and T_3 generation homozygous transgenic lines of *A. thaliana* were disinfected, vernalized at 4°C for 3 days, grown on Fe sufficient (+ Fe: 40 μM Fe) MS subculture medium for 10 days, then transferred to Fe deficient (-Fe: 0 μM Fe) MS medium for 20 days. Seedlings were placed in a light incubator (light 16 h/dark 8 h, 22°C). Fe was provided in the form of Fe-EDTA. The wild-type and transgenic apple calli were placed on MS (+ Fe: 40 μM Fe) succession medium containing 1.5 mg/L 2,4-D, 0.4 mg/L 6-BA for 10 days, and then transferred to Fe-deficient (-Fe:0 μM Fe) MS medium for 20 days.

The photosynthetic parameters (Pn, Gs, Tr, and Ci) were measured on leaves using a portable photosynthesizer (LI-6400, LI-COR, Linco ln, NE, USA), with each treatment being replicated three times.

The fluorescence parameters were assayed by IMAG-ING-PAM chlorophyll fluorescence imager which was measured at the same time as the photosynthetic parameters, then through 30 min dark treatment, and the fluorescence parameters F0, Fm, Fv/Fm, and qP were analyzed by Imaging Win Geg E soft-ware software.

The chloroplast pigment content, including chlorophyll a (Chla), chlorophyll b (Chlb), chlorophyll a + b (Chl a + b), and carotenoids (Car), was determined following the method described by Fitter et al.[37]. The activities of superoxide dismutase (SOD), peroxidase (POD) and catalase (CAT) were determined using a spectrophotometry kit from Suzhou Keming Biological (China).

The NBT and DAB staining was performed using the method of Romero-Puertas et al.[38]. Finally, following the method of Schikora and Schmidt[39], content of ferric chelate reductase (FCR) was calculated from absorbance measurements at 520 nm. The total Fe content was measured in accordance with the method of Mandal et al.[40]. The soluble protein (SP) content was assayed by Caumas Brilliant Blue staining[41]. The content of soluble sugar (SS) and starch (St) in the leaves was determined using the Anthrone method [42]. Acidifcation analysis was based on the method of Zhao et al.[43].

Extraction of DNA from transgenic Arabidopsis thaliana and calli

The DNA of transgenic *Arabidopsis* and apple calli were extracted using the SteadyPure Plant Genomic DNA Extration kit (Accurate Biotechnology (Hunan) Co., Ltd).

Construction of pGBKT7- MhLHCB15 bait vector

The specific primers *MhLHCB15*-BD (Table S1) were designed. The cDNA of *M. halliana* served as the template for amplification using RT-PCR, and the resultant product underwent purification and sequencing. The pGBKT7 vector was double digested with EcoR Ⅰ and Sal Ⅰ, and the correctly sequenced PCR purified and recovered products were ligated with the digested products to transform into *E.coli.* Subsequently, a single clone was picked for colony PCR detection, after conducting sequencing on the positive clones, we proceeded to extract the recombinant plasmid pGBKT7-*MhLHCB15* once the sequencing results were confirmed as accurate.

Decoy carrier self-activation assay

PGBKT7-*MhLHCB15* and empty pGADT7 were transferred into yeast Y2H Gold, coated on SD/-Trp-Leu solid medium, incubated inverted at 30℃ for 2 d and then streaked on SD/-Leu-Trp-His-Ade solid medium, incubated at 30 ℃ for 3–5 d to observe the growth of yeast colonies.

Interaction validation of the interaction proteins MhSGR1 and MhTHF1 with MhLHCB15

The pGADT7-*MhSGR1* and pGADT7-*MhTHF1* vectors were simultaneously introduced into yeast Y2H Gold cells along with pGBKT7-*MhLHCB15*, individually, and set up two negative controls (pGADT7 + pGBKT7-*MhLHCB15*, and pGBKT7 + pGADT7-*MhSGR1* and pGADT7-*MhTHF1*) coated on SD/-Trp-Leu

plate growth. The transformation solution was diluted 10-fold and divided into two parts. The transformation solution was diluted 10, 100 and 1,000 times and then spotted on SD/-Trp/-Leu/-His/-Ade/X-α-Gal plates and incubated for 3–5 days. The growth of yeast colonies and the color development were observed to verify the interactions between *MhLHCB15* and the interacting proteins, *MhSGR1* and *MhTHF1*.

Statistical analyses

For this study, treatment effects were evaluated through the use of analysis of variance. Means were then compared using Duncan's test ($P < 0.05$). Statistical analyses were carried out using SPSS version 22.0 and figures were created using Origin 8.0 software.

RESULTS

Identification of the MhLHC family members in apple and analysis of the physicochemical properties

A total of 33 typical *MhLHC* genes were derived using the apple genome database. They were named *MhLHCA1* to *MhLHCA10* and *MhLHCB1* to *MhLHCB22* on the basis of their chromosomal locations and known LHC genes in *Arabidopsis*. As shown in Table S2, the number of encoded amino acids was relatively equal with an average of 265.12. Isoelectric points (pIs) of the proteins were in the scope of 4.54 to 9.46, aliphatic indices ranged from 74.14 to 99.57, and molecular masses (MW) covered the range of 6272.21 to 38200.48 Da. The positive residues are between 5 to 33, and negative residues span from 5 to 34. Subcellular structural localization predictions revealed that all 33 LHC family proteins were located in chloroplasts.

Evolutionary relationships, structure and conserved motif of apple LHCB members

The phylogenetic analysis of 33 *MhLHC* protein sequences illustrated that the gene family can be categorized into three groups: Group I, Group II, and Group III (Fig. 1a). The results of the conserved motif analysis indicated all of Group □ contained motif 1 to motif 10, and both Group □ and Group □ contained motif 1, motif 2, motif 4, motif 6, and motif 7 (Fig. 1b). There are at least two introns for *MhLHCB1*, *MhLHCB6*, *MhLHCB2*, *MhLHCB9*, *MhLHCA1*, *MhLHCA2*, *MhLHCA3*, *MhLHCA6*, and *MhLHCA9*, while *MhLHCB8*, *MhLHCB7*, *MhLHCB16*, *MhLHCB15*, *MhLHCB21*, MhLHCB13, *MhLHCB20*, and *MhLHCB10* contain only one exon (Fig. 1c).

Chromosome distribution and collinearity analysis of the apple MhLHC genes

The chromosome location indicated that the apple *MhLHC* gene was asymmetrically distributed on 18 chromosomes (Fig. 2a). 5 *MhLHC* genes were located on the Chr17, with the maximum number, which was followed with 3 *MhLHC* genes, including in Chr05, Chr07 and Chr09, and lastly 2 *MhLHC* genes on Chr06, Chr08, Chr10 and Chr15. There were 10 covariant gene pairs between *MhLHC* genes (Fig. 2b),

which deserves special attention is the covariance of the *MhLHCB11*, *MhLHCB4* and *MhLHCB17* genes. Simultaneously, *MhLHCA10*, *MhLHCB20*, *MhLHCB23*, *MhLHCB22* have co-linear relationship with *MhLHCB7*, *MhLHCB8* and *MhLHCA5*, *MhLHCB14*, respectively. In addition, *MhLHCB3* and *MhLHCB10*, *MhLHCA9* and *MhLHCA6*, *MhLHCB21* and *MhLHCB13* have covariate relationships. Moreover, there was a covariance between *MhLHCA7* and *MhLHCA2*, *MhLHCB19* and *MhLHCB12*, *MhLHCA8* and *MhLHCA4*, and *MhLHCB18* with *MhLHCB5*, for each of them. The findings presented in this study reveal that the production of *MhLHC* genes could potentially arise from gene duplication occurrences, which segmental duplication events acted as an impelling role in the evolution of *MhLHC* proteins.

Phylogenetic analysis of LHC family members

Aiming to explore the putative function of the predicted *M. halliana* LHC, we allocated them to *Arabidopsis* LHC proteins with known functions. A total of 33 *MhLHC* proteins in *M. halliana* and 19 *AtLHC* proteins in *Arabidopsis* were analyzed. The phylogenetic tree was predicted using the Neighbor-Joining (NJ) method, followed by performing a Bootstrap analysis with 1000 replications (Fig. 3). The phylogenetic distribution indicated that the LHC proteins can be classified into 3 clades (named Group I, Group II, and Group III) according to the sequence similarity. Among them, Group □ is more distributed, which contains 31 members, Group □ includes 14 members, and Group I consists of the least number of members, with 7 members.

Analysis of cis-acting elements in promoter region of MhLHC gene

To comprehend the cis-acting elements contained in the promoter region of the apple *MhLHC* gene, 2-kbp sequences upstream of the *MhLHC* genes were taken and analyzed. The results demonstrated that multiple promoter regions of the *cis*-acting element-rich *MhLHC* genes were responsive to auxin, gibberellin, ABA, salicylic acid, MeJA, drought, low temperature, and light (Fig.S1), which suggested that the functions of the *MhLHC* may include a range of biological processes such as the regulation of plant growth and development, phytohormone signaling, and plant resistance to stresses.

Expression of apple MhLHC genes family members under different abiotic stresses

We selected 15 *MhLHC* genes that are homologous to respond to abiotic stresses in *Arabidopsis thaliana* and analyzed their relative expression under abiotic stresses such as Fe deficiency, drought, low temperature and saline-alkali, aiming to understand the expression patterns of apple *MhLHC* family genes under different abiotic stresses (Fig. 4). Among all *MhLHC* genes, *MhLHCB15, MhLHCA3, MhLHCA10* and *MhLHCB11* expression were remarkably up-regulated, with a maximum at 72 h under Fe deficiency, drought, low temperature and saline-alkali stress treatments compared to 0 h, of which *MhLHCB15* expression was markedly elevated. The expression of *MhLHCA1* and *MhLHCA7* genes were reduced under low temperature stress and saline-alkali stress, in which *MhLHCA7* expression was dramatically raised after 12 h of Fe deficiency and drought stress treatments. It indicates that there are differences in the response mechanisms to abiotic stresses among the genes of the *MhLHC* family, although most of the genes have similar response mechanisms to different abiotic stresses. To sum up,

the expression changes of other genes under abiotic stress were not as remarkable as those of *MhLHCB15* under Fe deficiency, which suggested that *MhLHCB15* might be involved in the response to Fe deficiency stress.

Analysis of the MhLHCB15 gene

The cDNA of *M. halliana* seedlings was used as template, and a 795 bp band was obtained (Fig.S2), encodes a total of 264 amino acids and possesses an isoelectric point of 5.29, thereby classifying it as an acidic protein. In addition, the positive and negative residues of *MhLHCB15* are 21 and 26, respectively, and the average hydrophobicity is -0.020, which is a hydrophilic protein (Table.S1). This indicates that the protein encoded by *MhLHCB15* is an acidic hydrophilic protein. Sequence alignment was carried out to compare the amino acid sequences encoded by *MhLHCB15* with those of other organisms, which showed a certain degree of difference at the N-terminal and high similarity at the C-terminal (Fig. 3). Phylogenetic analysis was performed on the amino acid sequences encoded by *MhLHCB1*5 and genes from similar species. *MhLHCB15* showed high homology to a protein from *Pyrus×bretschneideri* (97%) (Fig.S4).

The cis-elements in the sequence 2000 bp upstream of the *MhLHCB15* was analysed and multiple cis-elements associated with abiotic stress were found (Table 1), which suggests that *MhLHCB15* may exert a crucial part in response to diverse stresses.

Table 1
cis-elements in the genomic sequence 2000 bp upstream of the *MhLHCB15*

cis-acting element	Sequence	Start sites/bp	End sites/bp	Function
G-box	TACGTG	+ 601	+ 607	cis-acting regulatory element involved in light responsiveness
LTR	CCGAAA	+ 342	+ 348	cis-acting element involved in low-temperature responsiveness
ABRE	ACGTG	+ 602	+ 607	cis-acting element involved in the abscisic acid responsiveness
AuxRR-core	GGTCCAT	+ 1451	+ 1458	cis-acting regulatory element involved in auxin responsiveness
P-box	CCTTTTG	+ 1278	+ 1285	gibberellin-responsive element
ARE	AAACCA	-1067	-1073	cis-acting regulatory element essential for the anaerobic induction
MBS	CAACTG	+ 1334	+ 1340	MYB binding site involved in drought-inducibility
TGACG-motif	TGACG	-655	-660	cis-acting regulatory element involved in the MeJA-responsiveness

Identification of overexpressing A. thaliana and apple calli

The DNA of transgenic *A. thaliana* and overexpressed apple calli were extracted and characterized by PCR. As shown in the Fig. 5a-b, and the size of the detected electrophoretic bands is consistent with the size of the *MhLHCB15* fragment. The expression levels of *MhLHCB15* in transgenic *A. thaliana* and overexpressed apple calli were detected by qRT-PCR. In comparison to the plants with WT plants, the expression levels of *MhLHCB15* were higher in transgenic *A. thaliana* and overexpressed apple calli, indicating that *MhLHCB15* was overexpressing (OE) in both (Fig. 5c-d).

Tolerance of MhLHCB15 overexpressing A. thaliana to Fe deficiency

To determine whether *MhLHCB15* plays a role in response to Fe deficiency, three transgenic *A. thaliana* lines (OE-1, OE-2, OE-4) and the wildtype (WT) control were grown for 30 days under Fe-sufficient conditions, then shifted to Fe-sufficient or Fe-deficient conditions for another 20 days. This is shown in Fig. 6, *Arabidopsis* grew vigorously in normal conditions, and the growth rate was basically the same, while growth was inhibited to varying degrees when exposed to Fe-deficiency stress. Compared with transgenic *Arabidopsis*, WT control showed more obvious chlorosis and wilting.

As shown in Fig.S5, the three transgenic lines exhibited a remarkable increase in chl a, chl b car and chl a + b under Fe-deficient conditions when compared with WT, whereas they did not differ from WT under Fe-sufficient conditions. As can be seen from Fig. 7a-d, Tr, Gs and Pn of leaves showed a continuous decrease after Fe deficiency, though it was higher in transgenic plants compared to WT. However, the Ci content tended to be elevated, and the increase was more pronounced in the *MhLHCB15*-OE plants. The qP, F0, Fm, and Fv/Fm of both transgenic and WT plants exhibited a declining trend under Fe deficiency, which was lower in transgenic plants (Fig. 7e-h). The SOD, POD and CAT activities of transgenic and WT *A. thaliana* have been measured (Fig.S5e-g). Under Fe-deficient conditions, all measured parameters (SOD, POD and CAT) were much higher in transgenic *A. thaliana* than in WT controls. In addition, both Pro and MDA were remarkably elevated under Fe deficiency, and the Pro content was greater in the *MhLHCB15-OE A. thaliana* than in the WT strain, while the MDA content was also below that of the WT (Fig.S5h-i). The accumulation of H_2O_2 and O_2^- in *transgenic Arabidopsis* leaves in Fe-deficient conditions was significantly lower than that of the WT, with no obvious difference under normal conditions (Fig. 8a-b, Fig.S6a-b). The results demonstrated that the Fe^{2+} content and FCR activity were substantially higher than those of the WT control (Fig. 8c-d). Eventually, the content of soluble sugars, starch and soluble proteins was reduced in Fe deficiency, whereas it was greater in transgenic plants than in WT (Fig.S6c-e).

To further investigate the role of *MhLHCB15* in the Fe signaling pathway, the expression levels of Fe uptake-related genes in *Arabidopsis* plants overexpressing *MhLHCB15* were examined by qRT-PCR (Fig.S7). The results illustrated that the expression levels of Fe uptake-related genes (*AtAHA2*, *AtAHA8*, *AtFRO2*, *AtIRT1* and *AtFIT*) were decreased in overexpressed *Arabidopsis* plants under Fe deficiency stress, but the expression of *MhLHCB15*-OE was higher than that of WT. All the above results indicated that *MhLHCB15* enhanced the tolerance of *A. thaliana* under Fe deficient stress.

Tolerance of MhLHCB15 overexpressing apple calli to Fe deficiency

It is clear from Fig. 9a-b that there was no apparent difference in the growth status of overexpressed and WT apple calli under Fe-sufficient conditions. Nevertheless, the growth status of overexpressed and WT apple calli varied greatly under Fe deficient conditions, and the transgenic calli performed better than the WT apple calli.

In addition, the POD, SOD, and CAT activities of transgenic lines (OE-2, OE-5, and OE-7) diverse from those of WT tobacco under Fe deficiency stress, whose enzyme activities were considerably higher than those of the WT (Fig.S8a-c). In parallel, the transgenic lines Pro content was more than that of WT, while the MDA content was remarkably inferior to that of WT (Fig.S8d-e). It is evident from Fig.S8f-g that the accumulation of H_2O_2 and O_2^- in transgenic *Arabidopsis* leaves was markedly less than that of the WT at Fe deficiency, which was not appreciably dissimilar under normal conditions. Meanwhile, the transgenic lines with higher values of FCR activity and total Fe content when compared to the WT control lines (Fig. 9c-d). It is obvious from Fig.S8h-j that soluble sugar, starch, and soluble protein contents of transgenic *Arabidopsis* leaves dropped significantly when exposed to Fe deficiency, whereas the transgenic plants were notably superior to those of the WT. Additionally, bromocresol violet staining in yellow indicated that the *MhLHCB15* transgenic calli pumped more H^+ into the medium under Fe deficient conditions compared with the WT control (Fig. 10).

With a view to exploring further the role of *MhLHCB15* in the Fe signaling pathway, the expression levels of Fe uptake-related genes were assayed in apple calli overexpressing *MhLHCB15* by qRT-PCR (Fig. S9). In a word, these results demonstrate that homologous expression of *MhLHCB15* in apple calli can respond to Fe deficiency and reinforce its tolerance to stress.

Construction of decoy vectors pGBKT7- MhLHCB15 and self-activation assays

The results showed successful amplification of the target bands of approximately 795 bp (Fig.S10), which indicated he successful construction of the recombinant bait vector pGBKT7-MhLHCB15. The bait vector and positive control were then transferred into yeast Y2H Gold receptor cells to verify the self-activation activities. It showed that the bacterial fluids containing the bait vector and the positive control could grow normally in SD/-Trp-Leu medium, but only the positive control had blue colonies in SD/-Trp-Leu/X-a-Gal medium, and the bait vector could not grow (Fig. 11), which demonstrated that the bait vector did not have self-activation activity, and it could be used for the screening of interacting proteins.

Yeast point-to-point hybridization to verify MhLHCB15 with MhSGR1 and MhTHF1

When the candidate interacting proteins *MhSGR1* and *MhTHF1* were co-transfected into yeast with pGBKT7-*MhLHCB15* bait vector, respectively, which displayed that all the colonies were able to grow on SD/-Trp/-Leu/-His/-Ade/X-α-Gal plates and turned blue (Fig. 11), thus further confirming that the two proteins interacted with the *MhLHCB15* proteins in yeast.

Discussion

Identification of the LHC gene family in M. halliana

The light trapping is the utmost crucial part of the photosynthesis process, and it is mediated by LHC[44], a plant-specific family of proteins that are mainly localized in the chloroplast-like vesicle membranes. They bind to the pigments to form the light-trapping pigment-protein complexes, which are involved in the collection and transport of light energy during photosynthesis[45]. The LHC gene family has been extensively studied in model plants such as *Arabidopsis* (*Arabidopsis thaliana* L.)[46] and rice (*Oryza sativa* L.)[47]. The LHC gene family is thought to be involved in the regulation of plant growth and development, repair of light damage in the photosynthetic system, as well as in the response to various adversity stresses[16,15,48]. The levels of gene expression for the majority of *ZmLHCA* and *ZmLHCB* genes in *Zostera marina* are reduced when exposed to salt and low-temperature stress, consequently impacting the process of photosynthesis[49]. In *Arabidopsis*, low concentrations of ABA promote the expression of *AtLHCB1-6*, while high concentrations inhibit the expression of *AtLHCB1-6* in response to the regulation of the external environment, especially adversity stress[50], and down-regulation of the expression of *AtLHC1-LHCB6* affects stomatal responses to ABA, thus leading to a decrease in the ability of plants to tolerate drought[26]. Nevertheless, the study of related LHCII proteins in resistance to stress and disease in *M. halliana* has not yet been reported.

In the present study, we investigated 33 members of the LHC gene family in apple based on the apple genome database and bioinformatics analysis. The 33 *MhLHC* genes exhibited some differences in their physical and chemical properties (Table.S2). In addition, many studies have shown that subcellular location is critical for the biological function of the identified sequences, especially functional sequences related to the regulation of gene expression[51]. Our study demonstrated that 33 *MhLHC* genes were predicted to be located in chloroplasts (Table.S2). Through phylogenetic tree analysis, 33 *MhLHC* genes was divided into three groups (Fig. 1a). To further determine the relationship between *MhLHC* genes in apple, the structure diagram of conserved elements was established by MEME software (Fig. 1b), 33 *MhLHC* genes have ten conservative motifs, which may lead to functional diversity[52]. Although the LHC proteins in apples vary in length, the clustered LHC proteins share the same protein motif location and gene structure. It is consistent with previous studies at LHC family in the kiwifruit[53], which indicated that this family is highly conserved during evolution. The LHC gene is more widely distributed on the apple genome and is most abundant on chr.17 (Fig. 2a). At last, 10 pairs of genes were identified with segmental duplications (Fig. 2b). These outcomes revealed that the duplication events may contribute to the evolution of *MhLHC* genes.

Overexpression of MhLHCB15 enhanced tolerance to Fe deficiency in transgenic A. thaliana and apple calli

Iron is an essential trace element for plant growth. Any defect in Fe availability leads to an Fe deficiency reaction that causes leaf chlorosis and disrupts photosynthesis, affecting plant growth and crop yield[4]. The LHC is widely involved in the capture and transfer of light energy, leaf development, maintenance of

vesicle membrane structure, and various stress responses[54,55]. For instance, overexpression of the LHCB2 gene in tobacco enhanced tolerance to low temperatures[29]. Fe deficiency induces phosphorylation of *HvLHCB1* proteins, leading to their migration from grana stacks to stroma thylakoid membranes, thereby optimizing the excitation balance between PSII and PSI[56]. To summarize, LHC has a vital function which regulates gene expression in response to environmental stresses.

In this study, we examined the expression patterns of 15 MhLHC genes in the leaves of *M. halliana* by qRT-PCR validation, in which the expression of *MhLHCB15* changed dramatically under Fe deficiency stress (Fig. 4). We obtained transgenic *A. thaliana* with ectopically expressed *MhLHCB15* and homologous overexpressed apple calli (Fig. 5). The chlorophyll is critical for the absorption, transmission, and transformation of light[57]. We found that the chlorophyll content (Chl a, Chl b, Car and Chl a + b) of transgenic *Arabidopsis* under Fe deficiency stress was remarkably higher than that of WT (Fig.S5a-d), which indicated that the photosynthetic system of WT plants was more sensitive to Fe deficiency. It has been shown that the factors affecting the efficiency of plant photosynthesis include stomatal limitation and non-stomatal limitation[58]. When Gs and Ci decreased at the same time, the decline in Pn was mainly caused by stomatal limiting factors, whereas if the decrease in Pn was accompanied by an increase in Ci, the main restricting factors for photosynthesis were non-stomatal factors[59]. In this work, Pn, Gs, and Tr decreased notably after Fe deficiency stress. On the contrary, Ci increased remarkably (Fig. 7a-d), which indicated that non-stomatal limitation under Fe deficiency stress was one of the main reasons for the decrease of Pn. The leaf chlorophyll fluorescence parameter can be used as an effective characterization to measure the strength of the plant's ability to respond to adversity stress[60,61]. This experiment showed that qP, F0, Fm, and Fv/Fm of transgenic *MhLHCB5*-OE leaves under Fe deficiency stress showed a continuous decreasing trend (Fig. 7e-h), illustrating that the PSII reaction centers of the plants received damage and the electron transfer rate of plant leaves slowed down under Fe deficiency stress, and the PSII damage in *MhLHCB5*-OE was comparatively milder than in WT. The SOD, CAT and POD in plants facilitate the scavenging of ROS, thereby reducing the extent of membrane damage[62]. In the present study, we revealed that the POD, SOD, and CAT activities of transgenic *Arabidopsis* and apple calli were remarkably higher than those of WT under Fe deficient conditions (Fig.S5e-g, Fig.S8a-c), which meant that the *MhLHCB5*-OE had a stronger ability to scavenge ROS than WT, thus maintaining the stability of the membrane system. The Pro, as a very critical osmotic regulator, acts to stabilize the plant cell structure[63]. The Pro content of *MhLHCB5*-OE exhibited an upslope after Fe deficiency stress (Fig.S5h, Fig.S8d), which demonstrated that Fe deficiency stress caused severe osmotic stress to plants, and a large amount of Pro was accumulated in the plant cells to regulate the osmotic stress injury. The magnitude of damage to the membrane system was detected by the MDA content, which can be inferred from the plant's stress tolerance[64]. Following Fe deficiency stress, the MDA levels in the transgenic lines exhibited a decrease when compared to the WT plants (Fig.S5i, Fig.S8e), which demonstrated less cell membrane damage and enhanced resistance in *MhLHCB15*-OE.

When plants are subjected to adversity, reactive oxygen species (ROS) are accumulated, thus disrupting cell membranes, and exocytosis of inclusions[65]. We observed that H_2O_2 and O_2^- accumulation in transgenic *Arabidopsis* leaves was markedly less than in WT under Fe deficiency, and these findings align with the outcomes obtained from staining experiments using DAB and NBT. (Fig. 8a-b, Fig.S6a-b), thus confirming that overexpression of *MhLHCB15* enhances ROS scavenging capacity. The Fe^{2+} content of leaves is a pivotal factor that influences the chlorophyll content and degree of chlorosis of new leaves[66]. We found that the Fe content of transgenic *Arabidopsis* and apple calli were obviously greater than that of WT under Fe deficiency stress (Fig. 8c, Fig. 9c), suggesting that *MhLHCB15* may modulate Fe uptake. In our study, transgenic lines had a stronger FCR activity than WT (Fig. 8d, Fig. 8d), which may be attributed to the fact that *MhLHCB15* can promote Fe^{3+} reduction and enhanced iron utilization by increasing FCR activity. This study also demonstrated that overexpressed apple calli pumped out more protons (H^+) by acidification analysis (Fig. 10). It showed that overexpressed apple calli may elevate the activity of the H^+-ATPase and lower the pH, thereby raising the solubility of iron[67]. The soluble sugars and soluble proteins are essential signaling substances that are evoked to accumulate in plants in response to adversity stresses[68]. The findings revealed that the overexpressing lines accumulated more SS, St and SP contents than WT under Fe deficiency conditions, which indicated that the *MhLHCB15*-OE accumulated more osmoregulatory substances to alleviate the damages caused by Fe deficiency stress to the plants.

To further investigate the role of *MhLHCB15* in the signaling pathway of Fe deficiency stress, the expression levels of iron uptake-related genes (AHA2, AHA8, FRO2, IRT1 and FIT) in transgenic lines were assayed by qRT-PCR (Fig.S7, S9), and the expression of *MhLHCB15*-OE was higher than that of WT. All the above results indicated that *MhLHCB15* enhanced the tolerance of *A. thaliana* to Fe deficiency stress. Ultimately, the Y2H results demonstrated that *MhSGR1* and *MhTHF1* proteins interact with *MhLHCB15* protein (Fig.S11), which provides a robust theoretical basis for analyzing the construction of the regulatory network of *MhLHCB15* under Fe deficiency stress.

Conclusions

In conclusion, overexpression of the *MhLHCB15* gene enhances tolerance to Fe deficiency stress in *A. thaliana* by promoting the synthesis of photosynthetic pigments, elevating the activity of antioxidant enzymes and Fe^{3+} reduction; and overexpression of the *MhLHCB15* gene enhances tolerance to Fe-deficiency stress in apple calli by promoting the secretion of H^+ and reducing Fe^{3+}, while also boosting the activity of antioxidant enzymes. Overall, the overexpression of the *MhLHCB15* gene has been found to enhance tolerance to iron (Fe) deficiency stress in both *A. thaliana* and apple calli. The results of Y2H showed that *MhLHCB15* interacted with *MhSGR1* and *MhTHF1*. In the subsequent study, we will further confirm the interactions of *MhLHCB15* with *MhSGR1* and *MhTHF1* by using bimolecular fluorescence complementation (BiFC) and pulldown techniques, which will finally reveal the molecular mechanism of *MhLHCB15* in regulating Fe deficiency tolerance in apple.

Abbreviations

Amp Ampicilin

Car Carotenoid

CAT Catalase

cDNA Comolementary DNA

CDS Coding domain sequence

Cef Cefotaxime

Chl a Chlorophyll a

Chl a+b Chlorophyll a+b

Chl b Chlorophyll b

Ci Intercellular CO_2 concentration

DAB DAB Staining Sloution (Polymer)

EDTA Ethylenediamine tetraacetic acid

F0 Minimal fluorescence

FCR Ferric reductase activity

Fe Iron

Fm Fluorescence maximum

Fv/Fm Maximal photochemical efficiency of PS

H_2O_2 Hydrogen peroxide

IAA indole-3-acetic acid

Kan Kalamycin

LHCII light-harvesting chlorophyll a/b-binding protein

MDA Malondialdehyde

MS Murashige ang Skong medium

NBT Nitroblue tetrazolium chloride staining

O_2^- Superoxide anion

Pn Net photosynthetic rate

POD Peroxidase

Pro Proline content

PSI photosystem I

PSII photosystem II

qP Photochemical quenching coefficient

qRT-PCR Quantitative Reverse Transcriptio-PCR

Rif Rifampicin

ROS Reactive oxygen species

SOD Superoxide dismutase

SS Soluble protein

SS Sucrose synthetase

St Starch

SYBR Synergy brands

Tr Transpiration

WT Wild type

Y2H Yeast Two hybrid

Declarations

Acknowledgements

We thank Xiaofei Wang's laboratory at Shannon Agricultural University for the gift of the carrier.

Author contributions

YJD and YXW designed the research; YJD, DHZ and XYW performed the experiments; YJD and JC performed data analysis and interpretation; YLG and WBZ prepared the figures and tables; and YJD wrote the manuscript. All authors read, commented on and approved the final manuscript.

Funding

The National Natural Science Foundation of China (No.52169007).

Availability of data and materials

The raw data supporting the conclusions of this article will be made available by the authors, without undue reservation.

Ethics approval and consent to participate

We all declare that manuscript reporting studies do not involve any human participants, human data, or human tissue. So, it is not applicable. Experimental research and field studies on plants (either cultivated or wild), including the collection of plant material, must comply with relevant institutional, national, and international guidelines and legislation. No permission is required. Plants material was purchased.

Consent for publication

All authors listed have read the complete manuscript and have approved submission of the paper.

Competing interests

The authors declare that they have no competing interests.

References

1. Ryo T, Takehiro K, Shunpei I, Hana T, Kumiko I, Michika T. Systemic regulation of iron acquisition by *Arabidopsis* in environments with heterogeneous iron distributions. Plant And Cell Physiology. 2022;6(6).
2. Zargar SM, Agrawal GK, Randeep R, Yoichiro F. Quantitative proteomics reveals role of sugar in decreasing photosynthetic activity due to Fe deficiency. Frontiers in Plant Science. 2015; 6:592–595.
3. Fan P, Feng J, Jiang P, Chen X, Bao H, Nie L. Coordination of carbon fixation and nitrogen metabolism in *salicornia europaea* under salinity: comparative proteomic analysis on chloroplast proteins. Proteomics. 2011; 11(22):4346–4367.
4. Briat JF, Dubos C, Gaymard F. Iron nutrition, biomass production, and plant product quality. Trends in Plant Science. 2015;20(1):33–40.
5. Chen HM, Wang YM, Yang HL, Zeng QY, Liu YJ. Nramp1 promotes iron uptake at the late stage of iron deficiency in poplars. Tree Physiology. 2019;7(7).

6. Meral İ, Turgut YL, Önder T, Berken Ç. Differential tolerance to iron deficiency of citrus rootstocks grown in calcareous soil. Acta Horticulturae. 2015; 1065:1431–1436.
7. Zhang ZX, Zhang R, Wang SC, Zhang D, Zhao T, Liu B. Identification of *Malus halliana* R2R3-MYB gene family under iron deficiency stress and functional characteristics of *MhR2R3-MYB4* in *Arabidopsis thaliana*. Plant Biology. 2021.
8. Kawanabe S, Oshida T, Cheng ZT. Degeneration and conservational trial of Aneurolepidium chinense grassland in Northern China. Journal of Japanese Society of Grassland Science. 2017; 37:91–99.
9. Cheng L, Zhao T, Wu Y X, Wang H, Wang YX. Identification of AP2/ERF genes in apple (Malus × domestica) and demonstration that *MdERF017* enhances iron deficiency tolerance. Plant Cell Tissue and Organ Culture. 2020;143(2):465–482.
10. Dotaniya ML, Meena HM, Lata M, Kumar K. Role of phytosiderophores in iron uptake by plants. Agricultural Science Digest. 2013; 33(1):73–76.
11. Fernández V, Río V, Abadía J, Abadía A. Foliar iron fertilization of peach (*prunus persica (l.)* batsch): effects of iron compounds, surfactants and other adjuvants. Plant & Soil. 2006; 289(1–2):239–252.
12. Wang FP, Wang XF, Zhang JC, Ma FW and Hao YJ. *MdMYB58* modulates Fe homeostasis by directly binding to the *MdMATE43* promoter in plants. Plant & cell physiology. 2018; 59(12): 2476–2489.
13. Terry N, Abadia J. Function of iron in chloroplasts. J. Plant Nutr. 1986; 9:609–646.
14. Kale R, Hebert AE, Frankel LK, Sallans L, Bricker TM. Amino acid oxidation of the D1 and D2 proteins by oxygen radicals during photoinhibition of photosystem II. Proceedings of the National Academy of Sciences of the United States of America. 2017; 114:2988–2993.
15. Rochaix JD. Regulation and dynamics of the light-harvesting system, Annu. Rev. Plant Biol. 2014; 65:287–309.
16. Zhao S, Gao HB, Luo JW, Wang HB, Dong QL, Wang YP, Yang KY, Mao k,, Ma FW. Genome-wide analysis of the light harvesting chlorophyll a/b-binding gene family in apple (*Malus domestica*) and functional characterization of *MdLhcb4.3*, which confers tolerance to drought and osmotic stress. Plant Physiology and Biochemistry. 2020; 154:517–529.
17. Zhang Q, Ma C, Wang X, alma Q, Fan S, Zhang C. Genomewide identification of the light-harvesting chlorophyll a/b binding (LHC)family in Gossypium hirsutum reveals the influence of *GhLhcb2.3* on chlorophyll a synthesis. Plant Biology (Stuttgart, Germany). 2021; 23(5): 831–842.
18. Elias E, Liguori N, Saga Y, Schfers J, Croce R. Harvesting far-red light with plant antenna complexes incorporating chlorophyll a. Biomacromolecules, 2021; 22:3313–3322.
19. Najafpour MM, Allakhverdiev SI. Recent progress in the studies of structure and function of photosystems I and II. Journal of Photochemistry & Photobiology B Biology. 2015; 152:173–175.
20. Albanese P, Manfredi M, Meneghesso A, Marengod E, Saraccoe G, Barberf J, Morosinottob T, Paglianoa C. Dynamic reorganization of photosystem II supercomplexes in response to variations in light intensities. Biochimica et biophysica acta. Bioenergetics. 2016(1857): 1651–1660.

21. Aghdasi M, Schluepman H. Cloning and expression analysis cf two photosynthetic genes, PSI-H and LHCB1, under trehalose feeding conditions in *Arabidipsis* seedlings. Iranian Journal of Biotechnology. 2009;*7*(3):179–187 + 190.
22. Su X, Ma J, Wei X, Cao P, Zhu D, Chang W, Liu Z, Zhang X, Li M. Structure and assembly mechanism of plant C2S2M2-type PSII-LHCII super complex. Science. 2017; 357:815–820.
23. Zhu W, Xu L, Yu X, Zhong Y. The immunophilin CYCLOPHILIN28 affects PSII-LHCII super complex assembly and accumulation in Arabidopsis thaliana. Journal of Integrative Plant Biology. 2022; 64:915–929.
24. Yan M, Yuan Z. Genome-wide analysis of the family of light-harvesting chlorophyll a/b-binding proteins in pomegranate (*punica granatum* l.). Acta Horticulturae. 2020; 1297:647–652.
25. Xia Y, Ning Z, Bai G, Li R, Yan G, Siddique K. Allelic variations of a light harvesting chlorophyll a/b-binding protein gene (LHCB1) associated with agronomic traits in barley. Plos One. 2012;7(5).
26. Xu YH, Liu R, Yan L, Liu Z, Jiang SC, Shen YY, Wang XF, Zhang DP. Light-harvesting chlorophyll a/b-binding proteins are required for stomatal response to abscisic acid in *Arabidopsis*. Journal of Experimental Botany. 2012; 63(3):1095–1106.
27. Andersson J. Wentworth M, Walters RG, Howard CA, Ruban AV, Horton P, Jansson S. Absence of the lhcb1 and lhcb2 proteins of the light-harvesting complex of photosystem Ⅱ: Effects on photosynthesis, grana stacking and fitness. The Plant Journal. 2003; 35:350–361.
28. Jiang Q, Xu ZS, Wang F, Li MY, Ma J, Xiong AS. Effects of abiotic stresses on the expression of LHCB1 gene and photosynthesis of *oenanthe javanica* and *apium graveolens*. Biologia Plantarum. 2014; 58(2):256–264.
29. Deng YS, Kong FY, Zhou B, Zhang S, Yue MM, Meng QW. Heterology expression of the tomato LeLHCB2 gene confers elevated tolerance to chilling stress in transgenic tobacco. Plant Physiology & Biochemistry. 2014; *80*:318–327.
30. Fan P, Feng J, Jiang P, Chen X, Bao H, Nie L. Coordination of carbon fixation and nitrogen metabolism in *salicornia europaea* under salinity: comparative proteomic analysis on chloroplast proteins. Proteomics. 2011; 11(22):4346–4367.
31. Zhan J, Zhu X, Zhou W, Chen H, Wang Q. Thf1 interacts with PSI and stabilizes the PSI complex in *synechococcus sp*. pcc7942. Molecular Microbiology. 2016; 102(4):738–751.
32. Park SY, Yu JW, Park J S, Li J, Yoo SC, Lee NY. The senescence-induced staygreen protein regulates chlorophyll degradation. Plant Cell. 2007; 19:1649–1664.
33. Guo A, Hu Y, Shi MF, Wang H, Wang YX. Effects of iron deficiency and exogenous sucrose on the intermediates of chlorophyll biosynthesis in *Malus halliana*. PLoS One. 2020; 15(5).
34. Han ZH, Wang Q, Shen T. Comparison of some physiological and biochemical characteristics between iron-efficient and iron-inefficient species in the genus Malus. Journal of Plant Nutrition. 1994; 17:1257–1264.
35. Livak KJ, Schmittgen TD. Analysis of relative gene expression data using real-time quantitative PCR and the $2^{-\Delta\Delta Ct}$ method. Methods. 2001; 25:402–408.

36. Hu DG, Sun MH, Sun CH, Liu X, Zhang QY, Zhao J, Hao YJ. Conserved vacuolar H^+-ATPase subunit B1 improves salt stress tolerance in apple calli and tomato plants. Scientia Horticulturae. 2015; 197:107–116.
37. Fitter DW, Martin DJ, Copley MJ, Scotland RW, Langdale JA. GLK gene pairs regulate chloroplast development in diverse plant. The Plant Journal. 2010; 31:713–727.
38. Romero MC, Rodri SM, Corpas FJ. Cadmium-induced subcellular accumulation of O_2^- and H_2O_2 in pea leaves. Plant, Cell & Environment. 2004; 27(9):1122–1134.
39. Schikora A, Schmidt W. Iron stress-induced changes in root epidermal cell fate are regulated independently from physiological responses to low iron availability. Plant Physiology. 2001; 125:1679–1687.
40. Mandal Š, Banjanin B, Kujović I. Spectrophotometric determination of total iron content in black tea. Glas Hem Tehnol Bosne Hercegovine. 2015; 44(25):29–32.
41. Bradford MM. A rapid and sensitive method for the quantitation of microgram quantities of protein utilizing the principle of protein-dye binding. Anal Biochem.1976;72(1/2):248–254.
42. Wu M, Liu H, Gao Y, Shi Y, Xiang Y. The Moso bamboo drought-induced 19 protein phedi19-8 functions oppositely to its interacting partner, phecdpk22, to modulate drought stress tolerance. Plant Science. 2020; 299:110605.
43. Zhao Q, Ren YR, Wang QJ. Overexpression of *MdbHLH104* gene enhances the tolerance to iron deficiency in apple. Plant Biotechnol J. 2016; 14(7):1633–645.
44. Hey D, Grimm B. ONE-HELIX PROTEIN2 (OHP2) is required for the stability of OHP1 and assembly factor HCF244 and is functionally linked to PSII biogenesis. Plant Physiology. 2018; 177(4):1453–1472.
45. Alboresi A, Stefano C, Fabien N, Roberto B, Tomas M, Fugmann SD. In silico and biochemical analysis of Physcomitrella patens photosynthetic antenna: identification of subunits which evolved upon land adaptation. PLoS One.2008; 3(4):2033.
46. Zhao Y, Kong H, Guo Y L, Zou Z. Light-harvesting chlorophyll a/b-binding protein-coding genes in jatropha and the comparison with *Castor*, *Cassava* and *Arabidopsis*. Peer J. 2020; 8(4): e8465.
47. Pavan U. Genome-wide analysis of the family of light harvesting chlorophyll a/b-binding proteins in *Arabidopsis* and rice. Plant Signaling & Behavior. 2010; 5(12):1537–1542.
48. Singh J, Pandey P, James D, Chandrasekhar K, Achary VM, Kaul T, Tripathy BC, Reddy MK. Enhancing C3 photosynthesis: an outlook on feasible interventions for crop improvement, Plant Biotechnol J. 2014; 12(9):1217–1230.
49. Kong F, Zhou Y, Sun P, Gao M, Li H, Mao Y. Identification of light-harvesting chlorophyll a/b-binding protein genes of *Zostera marina* L. and their expression under different environmental conditions. J. Ocean Univ. China. 2016; 15:152–162.
50. Liu R, Xu YH, Jiang SC, Lu K, Lu YF, Feng XJ, Wu Z, Liang S, Yu YT, Wang XF, Zang D. Light-harvesting chlorophyll a/b-binding proteins, positively involved in abscisic acid signaling, require a transcription

repressor, WRKY40, to balance their function, J. Exp. Bot. 2013; 64:5443–5456.

51. Girardi CL, Rombaldi CV, Dal CJ, Nobile PM, Laurens F, Bouzayen M, Quecini V. Genome-wide analysis of the AP2/ERF superfamily in apple and transcriptional evidence of ERF involvement in *scab pathogenesis*. Scientia Horticulturae. 2013; 151:112–121.
52. Fujita Y, Yoshida T, Yamaguchi-Shinozaki K. Pivotal role of the AREB/ABF-SnRK2 pathway in ABRE-mediated transcription in response to osmotic stress in plants. Physiol Plant. 2013; 147:15–27.
53. Luo J, Abid M, Tu J, Gao P, Wang Z, Huang H. Genome-Wide Identification of the LHC Gene Family in Kiwifruit and Regulatory Role of AcLhcb3.1/3.2 for Chlorophyll a Content, Int. J. Mol. Sci. 2022; 23(12): 6528.
54. Myouga F, Takahashi K, Tanaka R, Nagata N, Kiss AZ, Funk C, Nomura Y, Nakagami H, Jansson S, Shinozaki K. Stable accumulation of photosystem II requires one-helix protein1 (OHP1) of the light harvesting-like family. Plant Physiol. 2018; 176(3):2277–2291.
55. Umate P. Genome-wide analysis of the family of light-harvesting chlorophyll a/b binding proteins in Arabidopsis and rice. Plant Signaling & Behavior. 2010; 5(12):1537–1542.
56. Saito A, Shimizu M, Nakamura H, Maeno S, Katase R, Miwa E. Fe deficiency induces phosphorylation and translocation of LHCB1 in barley thylakoid membranes. Febs Letters. 2014; 588(12):2042–2048.
57. Zuo Z, Chen Z, Zhu Y. Effects of NaCl and Na_2CO_3 stresses on photosynthetic ability of Chlamydomonas reinhardtii. Biologia. 2014; 69:1314–1322.
58. Farquhar GD, Sharkey TD. Stomatal conductance and photosynthesis. Annual Review of Plant Physiology. 1982;33(1):317–345.
59. Mafakheri A, Siosemardeh A, Bahramnejad B, Struik PC, Sohrabi Y. Effect of Drought Stress on Yield, Proline and Chlorophyll Contents in Three Chickpea Cultivars. Australian Journal of Crop Science. 2010; 4(8):580–585.
60. Ali S, Xu Y, Jia Q, Ma X, Ahmad I, Adnan M. Interactive effects of plastic film mulching with supplemental irrigation on winter wheat photosynthesis, chlorophyll fluorescence and yield under simulated precipitation conditions. Agricultural water management. 2018; 207:1–14.
61. Maxwell K, Johnson GN. Chlorophyll Fluorescence a Practical Guide. Journal of Experimental Botany. 2000; 51(345): 659–668.
62. Miller G, Suzuki N, Ciftciyilmaz S, Mittler R. Reactive oxygen species homeostasis and signaling during drought and salinity stresses. Plant Cell Env. 2010; 33:453–467.
63. Zhang LP, Wang XF, Shi QH. Differences of Physiological Responses of Cucumber Seedlings to NaCl and $NaHCO_3$ Stress. Chinese Journal of Applied Ecology. 2008; 19(8):1854–1859.
64. Tang LL, Cai H, Ji W, Luo X, Wang ZY, Wu J, Wang XD, Cui L, Wang Y, Zhu YM, Bai X. Overexpression of *GsZFP1* enhances salt and drought tolerance in transgenic alfalfa (*Medicago sativa* L.). Plant Physiol Biochem. 2013; 71(71):22–30.

65. Javaux M, Schroder T, Vanderborght J, Vereecken H. Use of a three-dimensional detailed modeling approach for predicting root water uptake. Vadose Zone Journal. 2008; 7 (3):1079–1088.
66. Incesu M, Turgut Y, Onder T, Berken Ç, Bilge Y. Response of citrus rootstocks to iron deficiency under high pH conditions. Citrus Research&Technology. 2016; 37:66–75.
67. Santi S, Schmidt W. Dissecting iron deficiency-induced proton extrusion in *Arabidopsis* roots. New Phytol. 2009; 183(4):1072–1084.
68. Rahdari P, Tavakoli S, Hosseini SM. Studying of salinity stress effect on germination, proline, sugar, protein, lipid and chlorophyll content in Purslane (*Portulaca oleracea* L.) leaves. J Stress Physiol Bioch. 2012; 8(1):182–193.

Figures

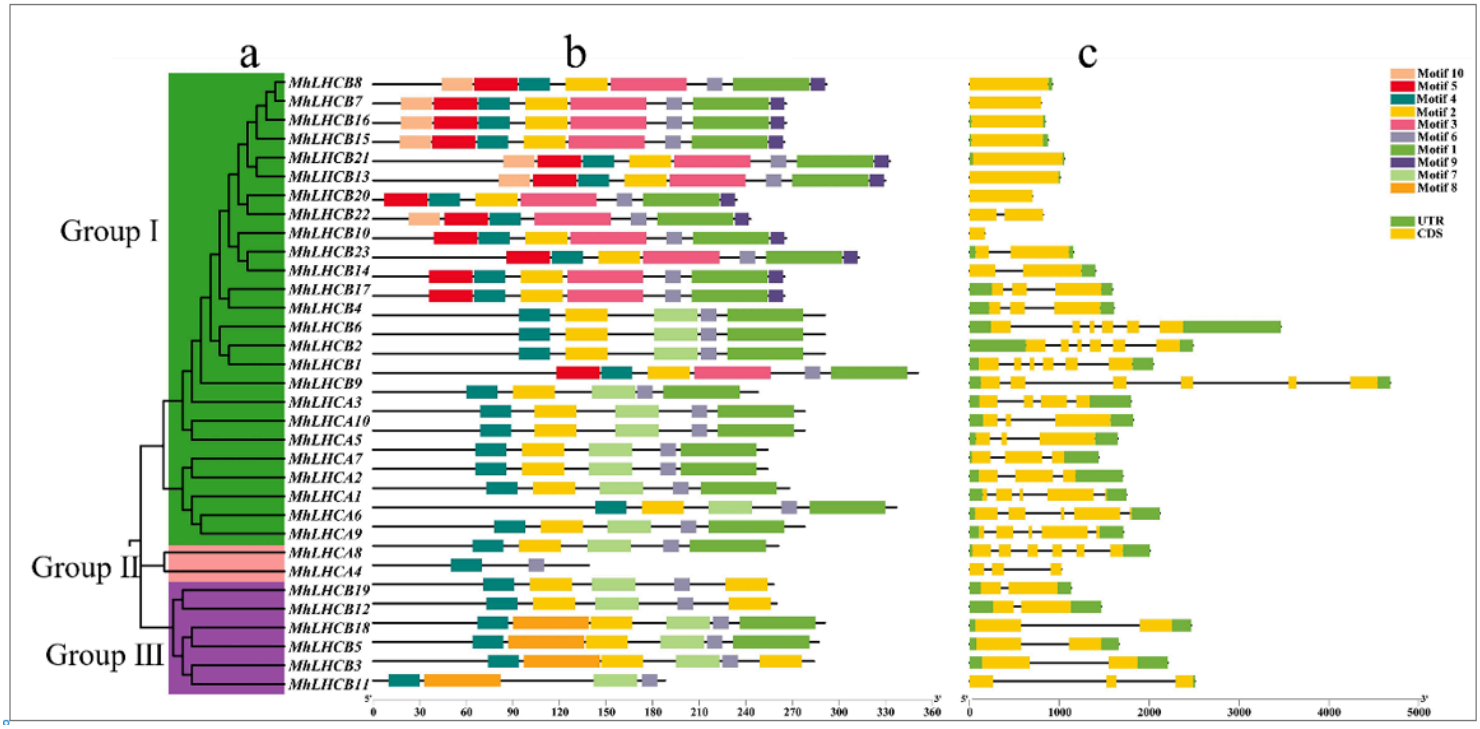

Figure 1

Phylogenetic relationships, architecture of conserved protein motifs, and gene structure in *MhLHC*gene family from apple. a The phylogenetic tree was constructed based on the full-length sequences of *MhLHC* family proteins using MEGA-X software. Details of clusters are shown in different colors. b The motif composition of *MhLHC*proteins. The motifs, numbers 1-10, are displayed in different colored boxes. The scale at the bottom can be used to estimate the length of the protein.. c Exon-intron structure of *MhLHC* genes family. Green boxes represent untranslated 5'- and 3'-regions; yellow boxes denote exons; black lines indicate introns.

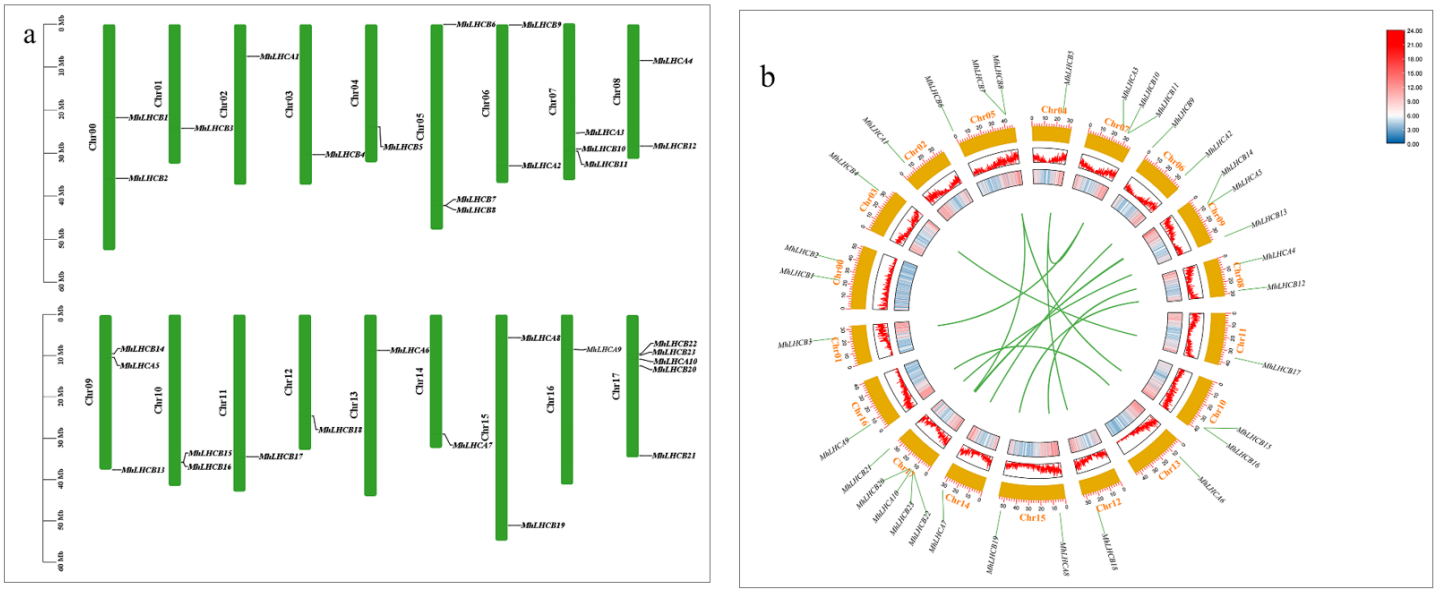

Figure 2

Chromosome locations and the collinearity analysis for *MhLHC*genes family. a Chromosome locations b collinearity analysis of *MhLHC*genes family. Thick green lines indicate duplicated *MhLHC* gene pairs. Gene names are shown in black font. Chromosome number is indicated at the bottom of each chromosome. Scale bars marked on each chromosome indicates chromosome length (Mb).

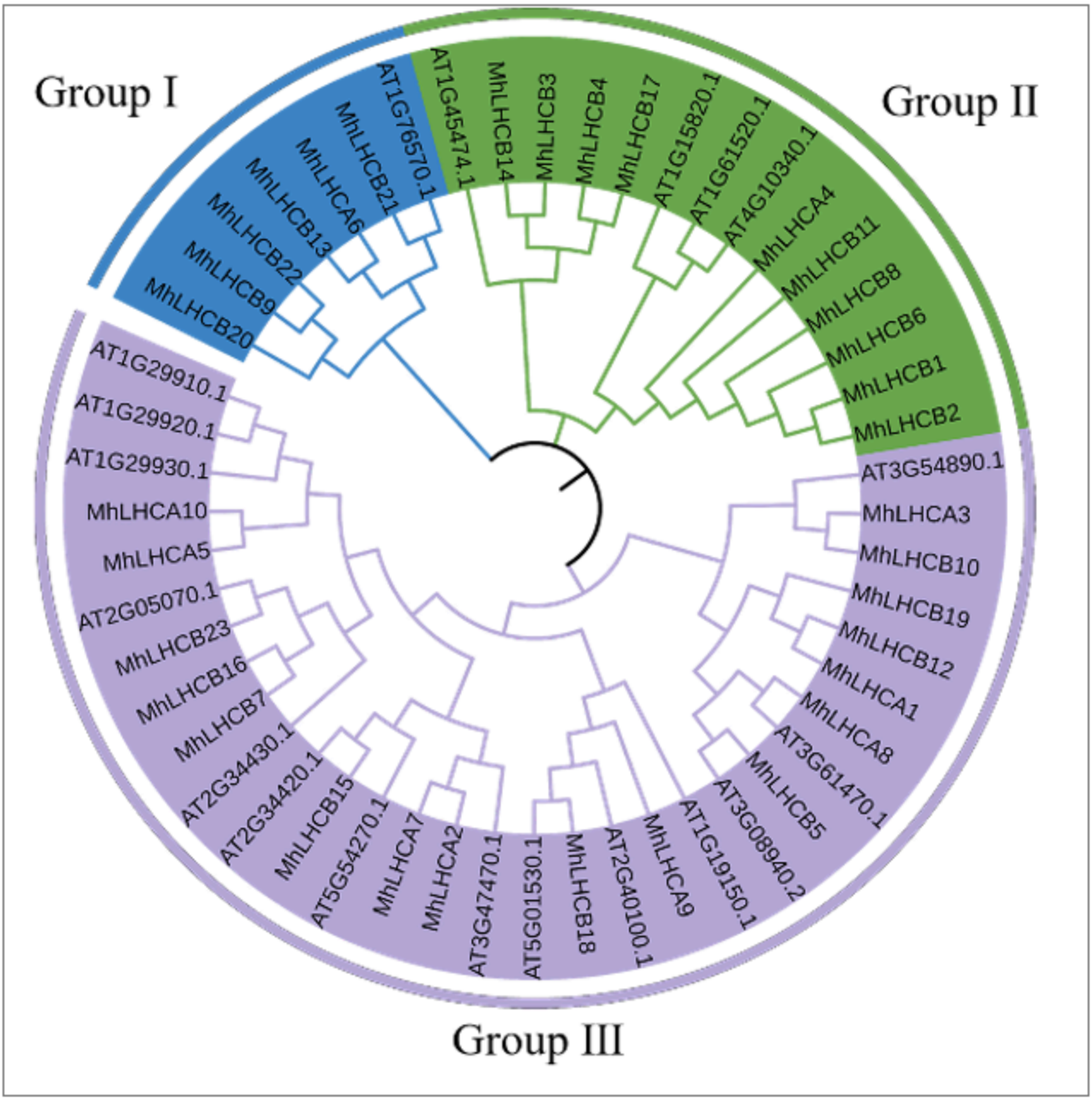

Figure 3

The phylogenetic tree of LHC proteins from *M. halliana* and *A. thaliana*.

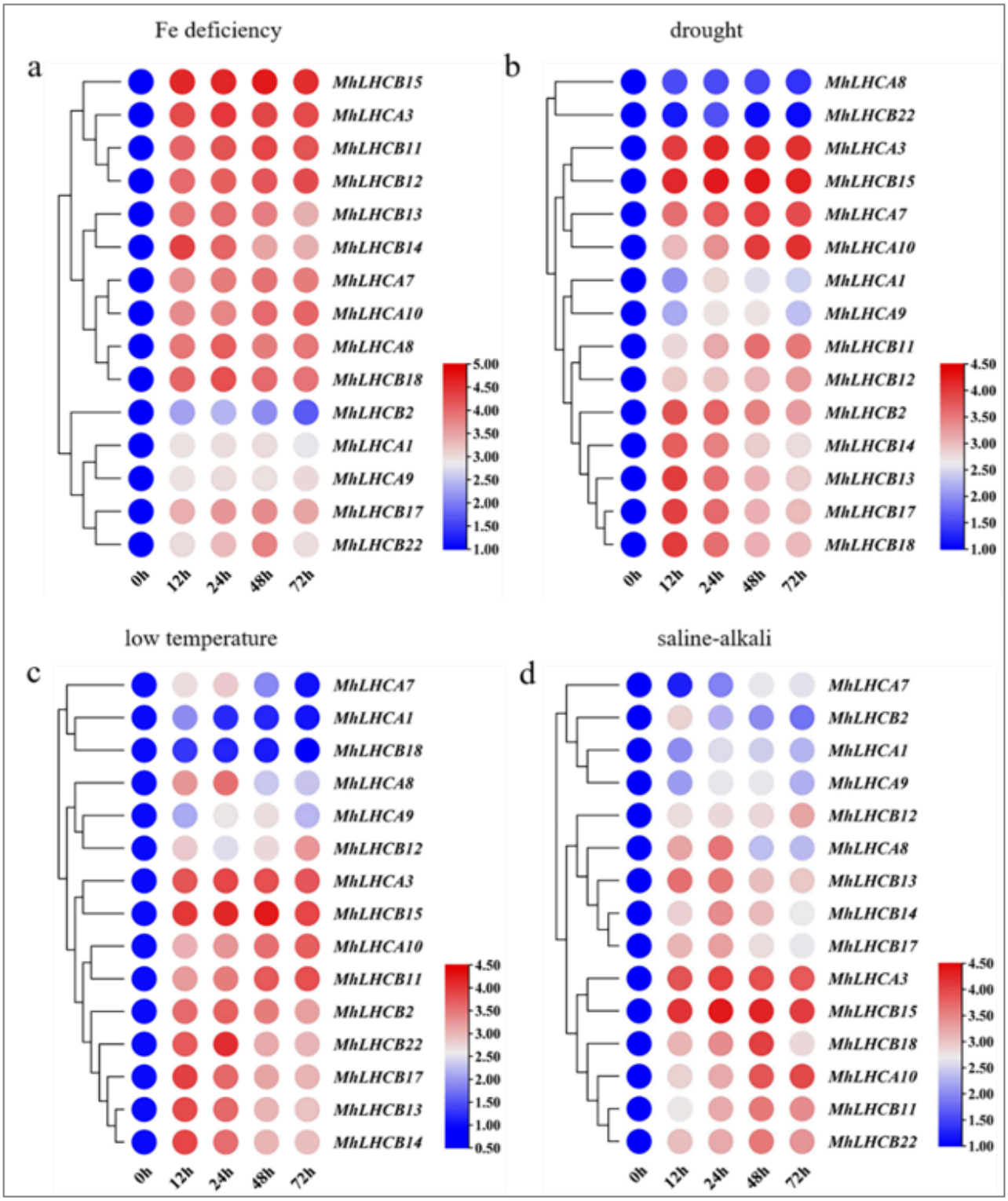

Figure 4

Heat map relative expression levels of *MhLHC* genes in *M. halliana* leaf cultures on abiotic stress medium at 0, 12, 24, 48 and 72 h. a Fe deficiency (0 μM Fe); b drought stress (15% PEG 6000); c low temperature (4°C); d saline-alkali stress (200 mmol/L NaCl+$NaHCO_3$).

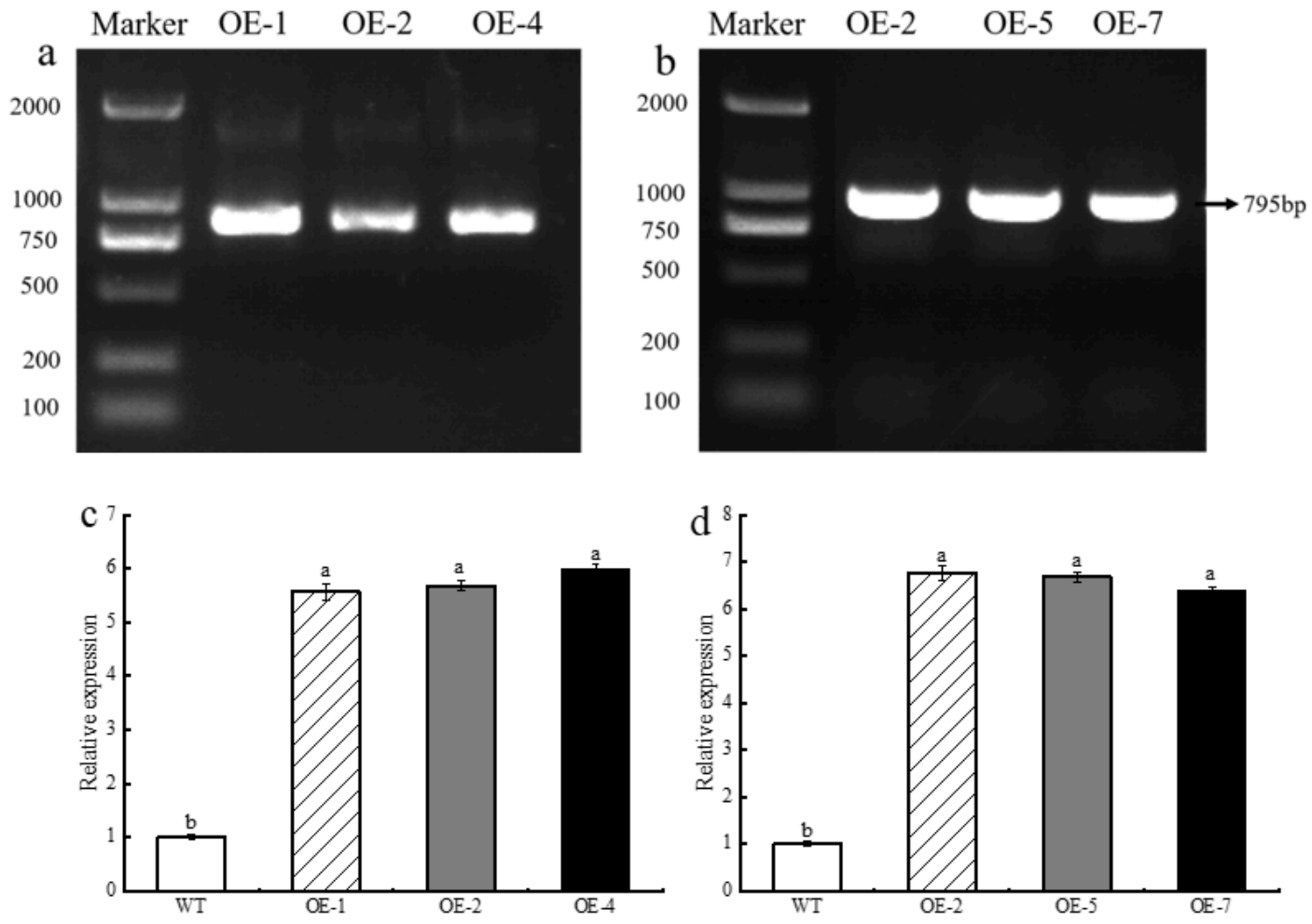

Figure 5

Identification of genetically modified material. a DNA identification of transgenic *A. thaliana*. b DNA identification of overexpressed apple calli. c Expression level of *MhLHCB15* in *A. thaliana*. d Expression level of *MhLHCB15* in apple calli. Resistance of transgenic *MhLHCB15 A. thaliana* and apple calli to Fe (iron) deficiency stress.

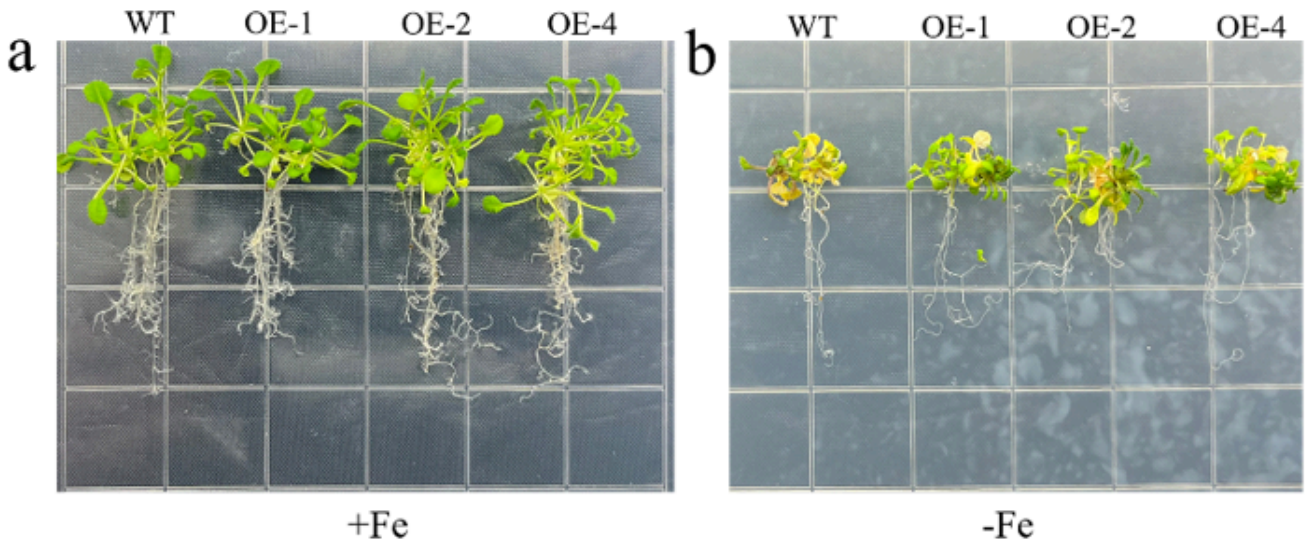

Figure 6

The phenotypes of *MhLHCB15*transgenic and wild-type (WT) *A. thaliana* grown for 20 days on Fe-sufficient or Fe-deficient medium. a Fe-sufficient; b Fe-deficient.

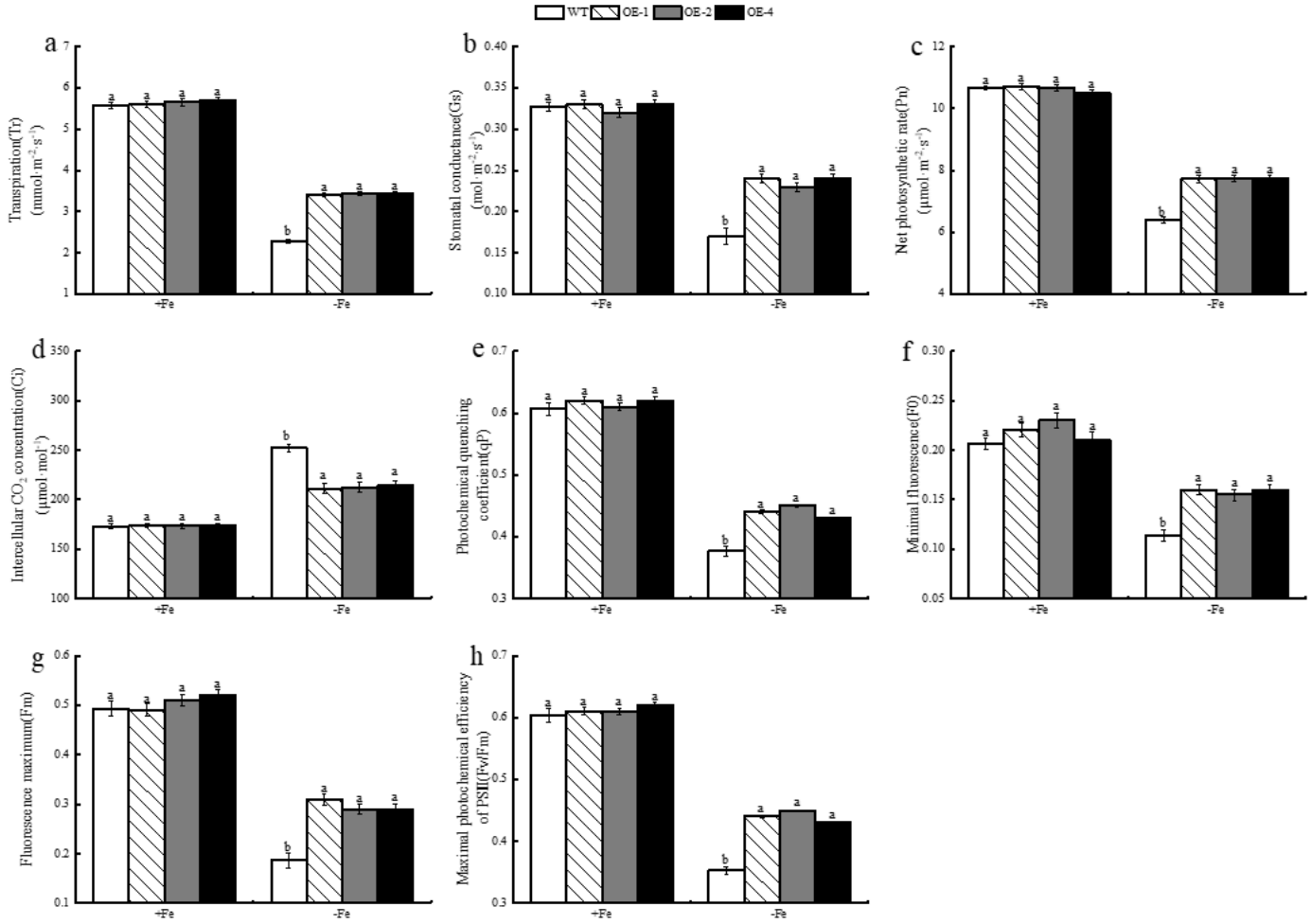

Figure 7

The photosynthetic characteristics and fluorescence parameters of wild type and *MhLHCB15* transgenic *Arabidopsis thaliana* grown for 20 days under Fe-sufficient(+Fe) or Fe-deficient(-Fe) conditions. a Transpiration (Tr); b Stomatal conductance (Gs); c Net photosynthetic rate (Pn); d Intercellular CO_2 concentration (Ci); e Photochemical quenching coefficient (qP); f Minimal fluorescence(F0); g Fluorescence maximum (Fm); h Maximal photochemical efficiency of PS□(Fv/Fm). Different lowercase letters showed significant difference at the level of P<0.05. The same below.

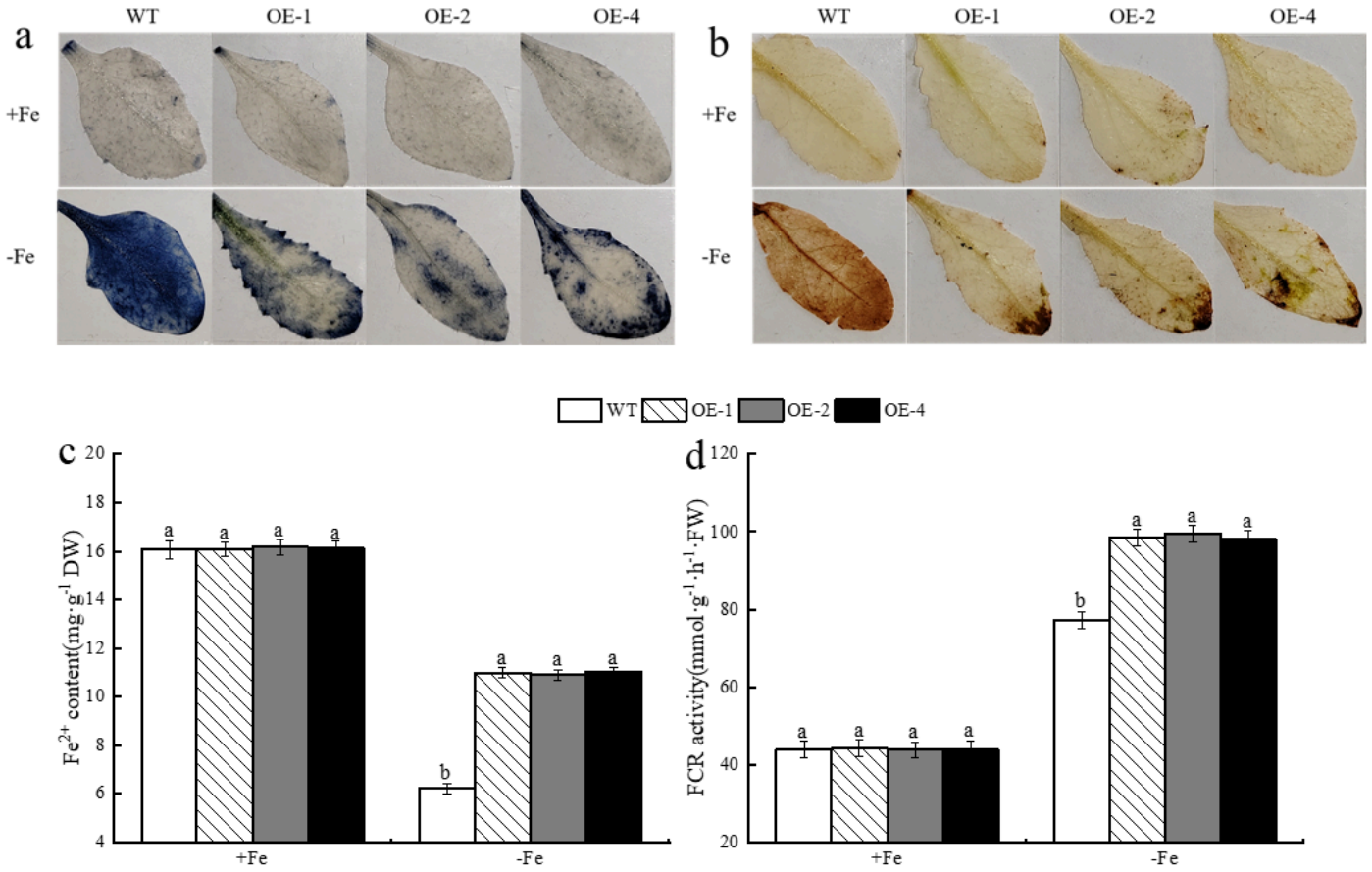

Figure 8

The Reactive oxygen species (ROS) analysis, Fe^{2+} content and FCR activity of wild type (WT) and *MhLHCB15* transgenic Arabidopsis thaliana grown for 20 days under Fe-sufficient (+Fe) or Fe-deficient (-Fe) conditions. a NBT staining; b DAB tissue staining; c Fe^{2+} content; d FCR activity.

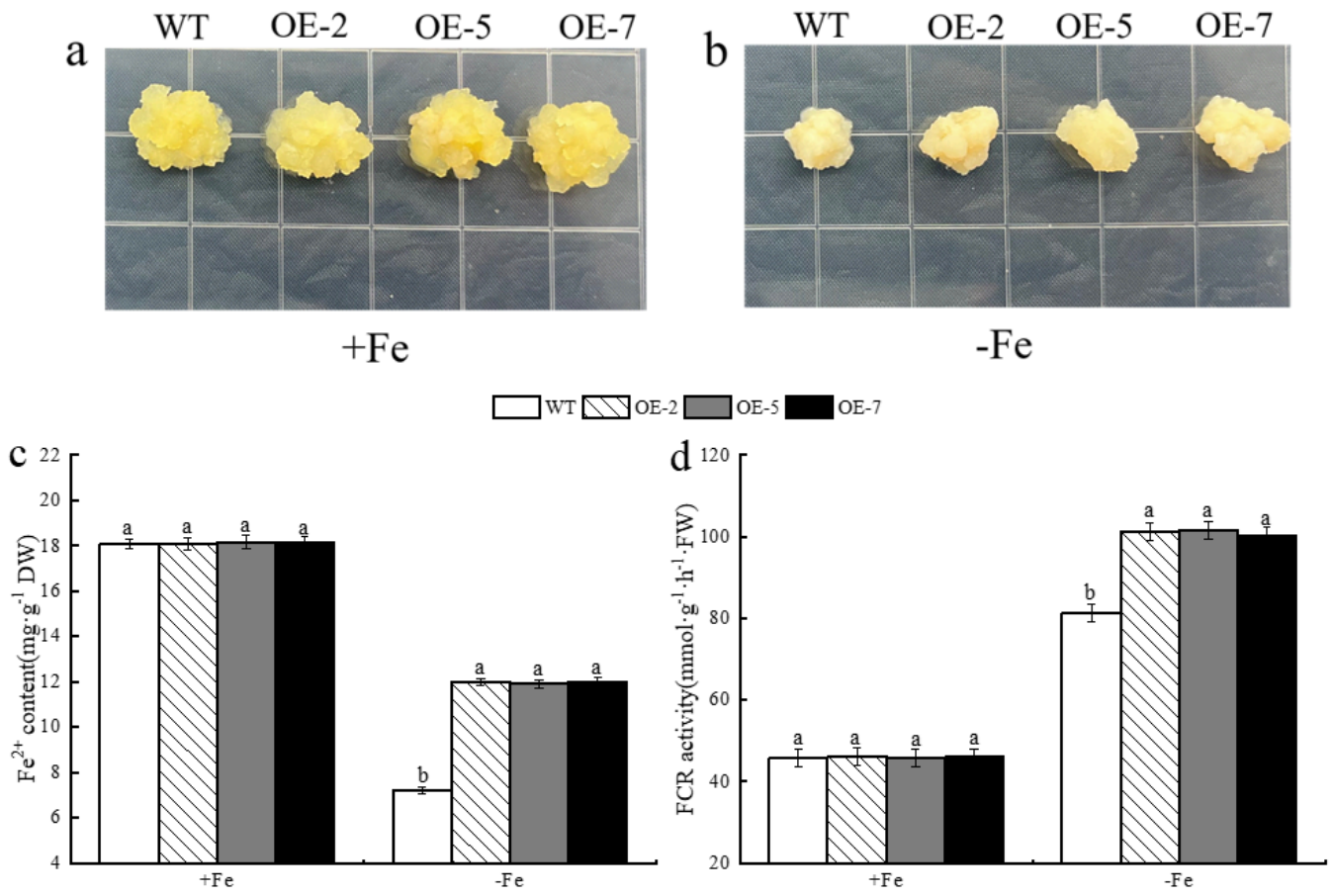

Figure 9

Phenotypes, Fe^{2+} content and FCR activity of *MhLHCB15* transgenic and wild-type (WT) control apple calli grown on Fe-sufficient or Fe-deficient media for 20 days. a Fe-sufficient; b Fe-deficient.

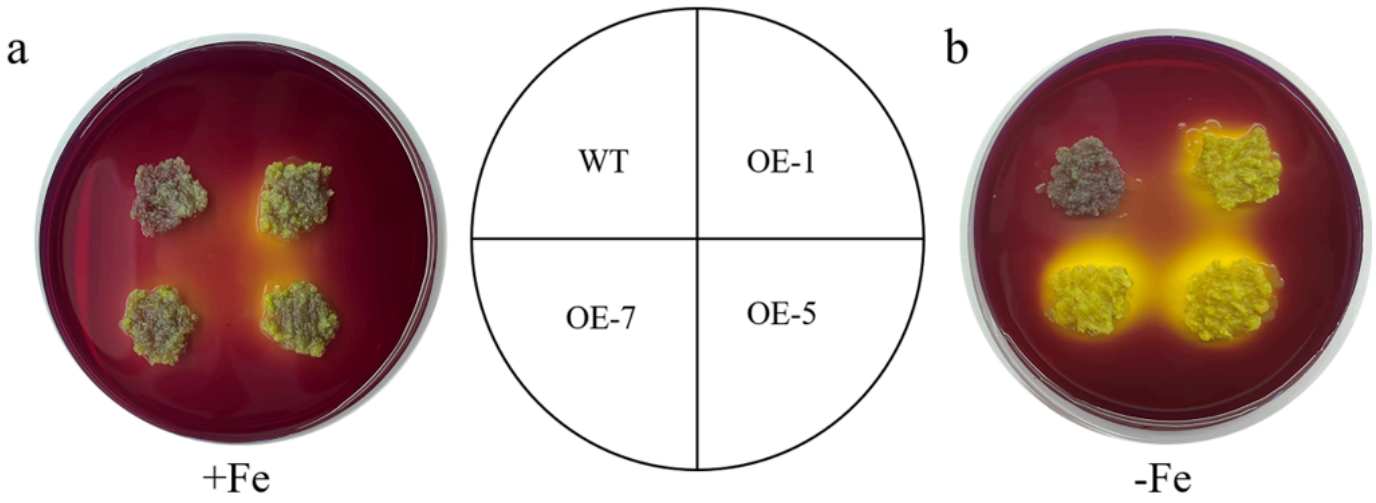

Figure 10

Acidifcation analysis of transgenic *MhLHCB15* apple calli on medium containing the pH indicator dye bromocresol violet. A yellow color around apple calli indicates acidification. a Fe-suficient. b Fe-deficient.

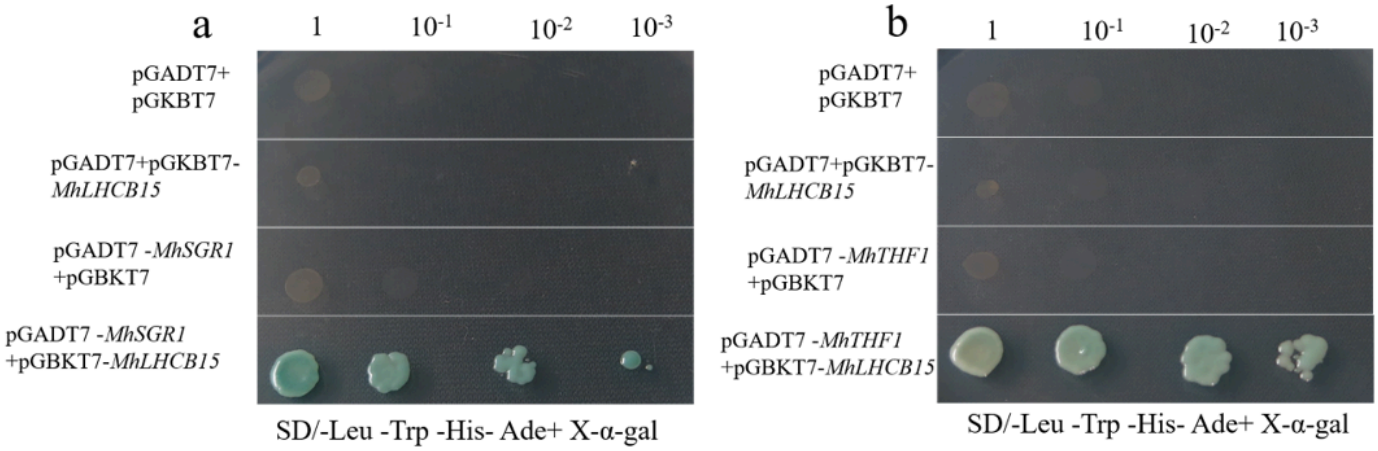

Figure 11

Identification of the interaction between *MhLHCB15* with *MhSGR1* and *MhTHF1*by Y2H assays.

Supplementary Files

This is a list of supplementary files associated with this preprint. Click to download.

- supplementarymaterial.docx
- GraphicalAbstract.png